Electronic Supplementary Material (ESI) for Journal of Materials Chemistry A.

Supporting Information

for

On the origin of non-monotonic variation of lattice parameters of $LiNi_{1/3}Co_{1/3}Mn_{1/3}O_2$ with lithiation/delithiation: a first-principles study

Liang-Yin Kuo,[a,b] Olivier Guillon,[b] and Payam Kaghazchi[*b]

[a]Physikalische und Theoretische Chemie, Freie Universität Berlin, Arnimallee 22, D-14195 Berlin, Germany

[b]Forschungszentrum Jülich GmbH, Institute of Energy and Climate Research, Materials Synthesis and Processing (IEK-1), D-52425, Jülich, Germany

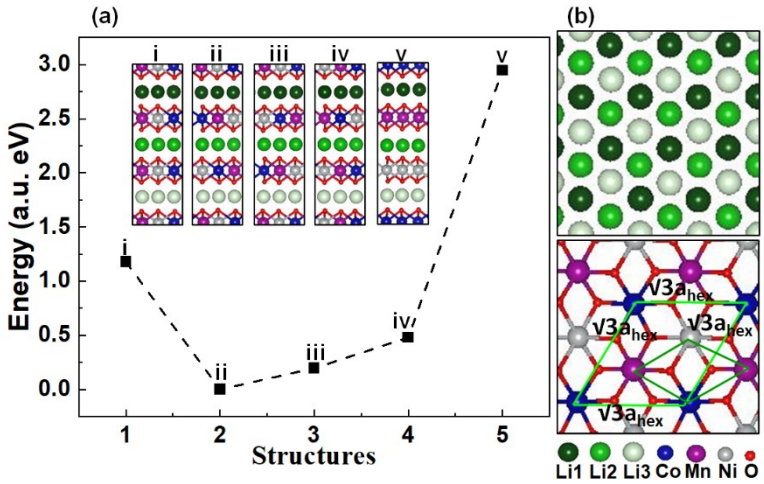

Figure S1. (a) Energy difference between NMC111 structures with various TM cations arrangements. (b) Top views of the Li and O–TM–O layers in the most favorable NMC111 structure (ii).

x	PBE	PBE+*U*	SCAN	Exp.
1.00	48.1	86.0	58.5	60
0.67	43.9	83.9	46.5	48
0.50	21.4	73.8	41.0	42
0.33	36.0	61.2	35.6	36
0.17	24.0	70.9	33.5	-

Table S1. Calculated total number of unpaired spins (NUS) for Li*x*NCM111 with *x*= 1.00, 0.67, 0.50, 0.33, and 0.17 using different types of XC functionals. Expected NUS values (based on previous experimental and theoretical studies) for a perfect ionic system are also listed.

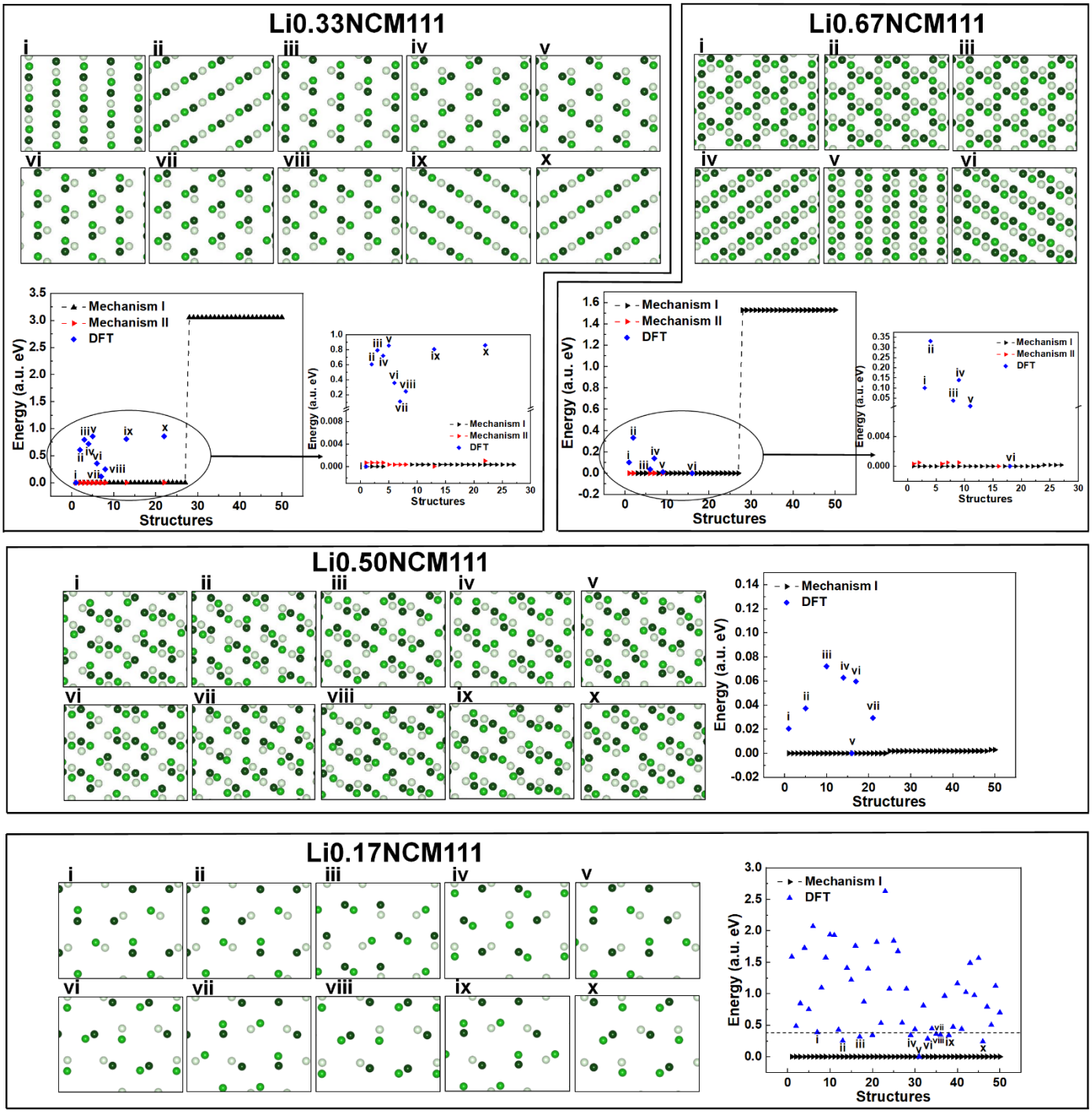

Figure S2. Calculated total Coulomb energies (referenced to the minimum energy) for Li*x*NCM111 (*x* = 0.67, 0.50, 0.33, and 0.17). Calculated DFT-PBE total energies of the most favorable structures based on the electrostatic analysis are also given. Arrangements of Li ions in several (DFT-PBE-calculated) lowest-energy structures are also presented.

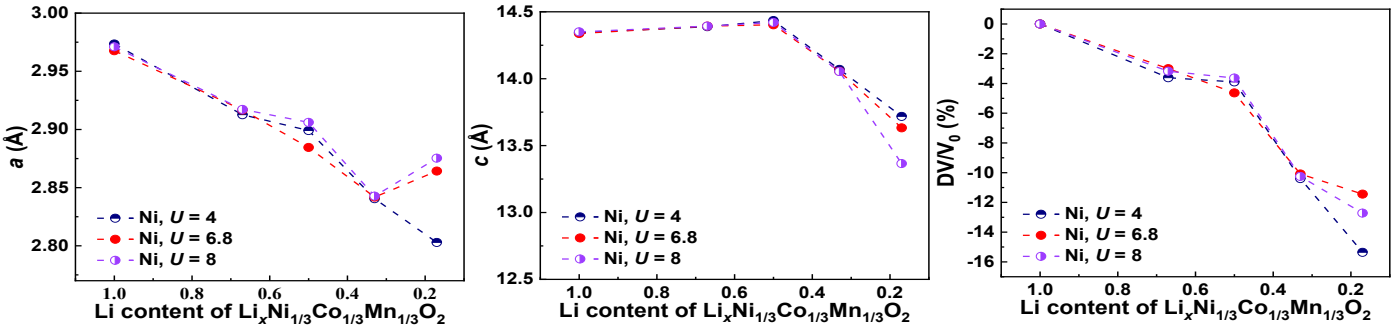

Figure S3. Calculated lattice parameters and volume change as function of *x* for Li*x*NCM111 using DFT-PBE+*U* with different *U* values for Ni.

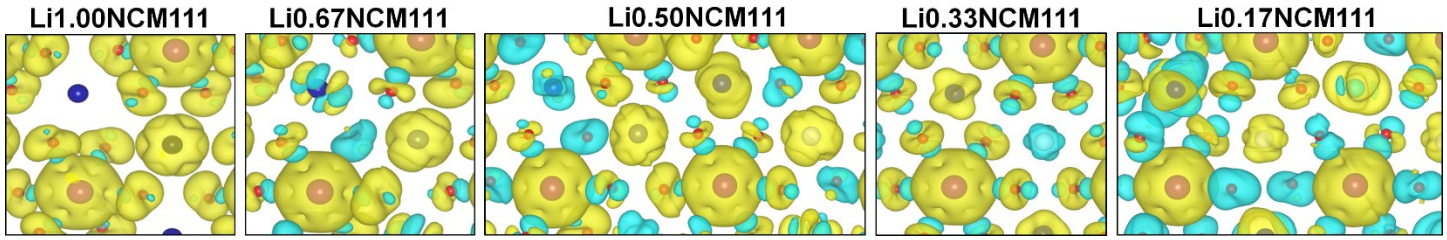

Figure S4. Calculated spin density difference (SDD) in the most favorable Li*x*NCM111 structures using the SCAN functional. Up-spin and down-spin electrons are in yellow and blue, respectively. An isosurface of 0.004 electrons/Å^3 was applied.

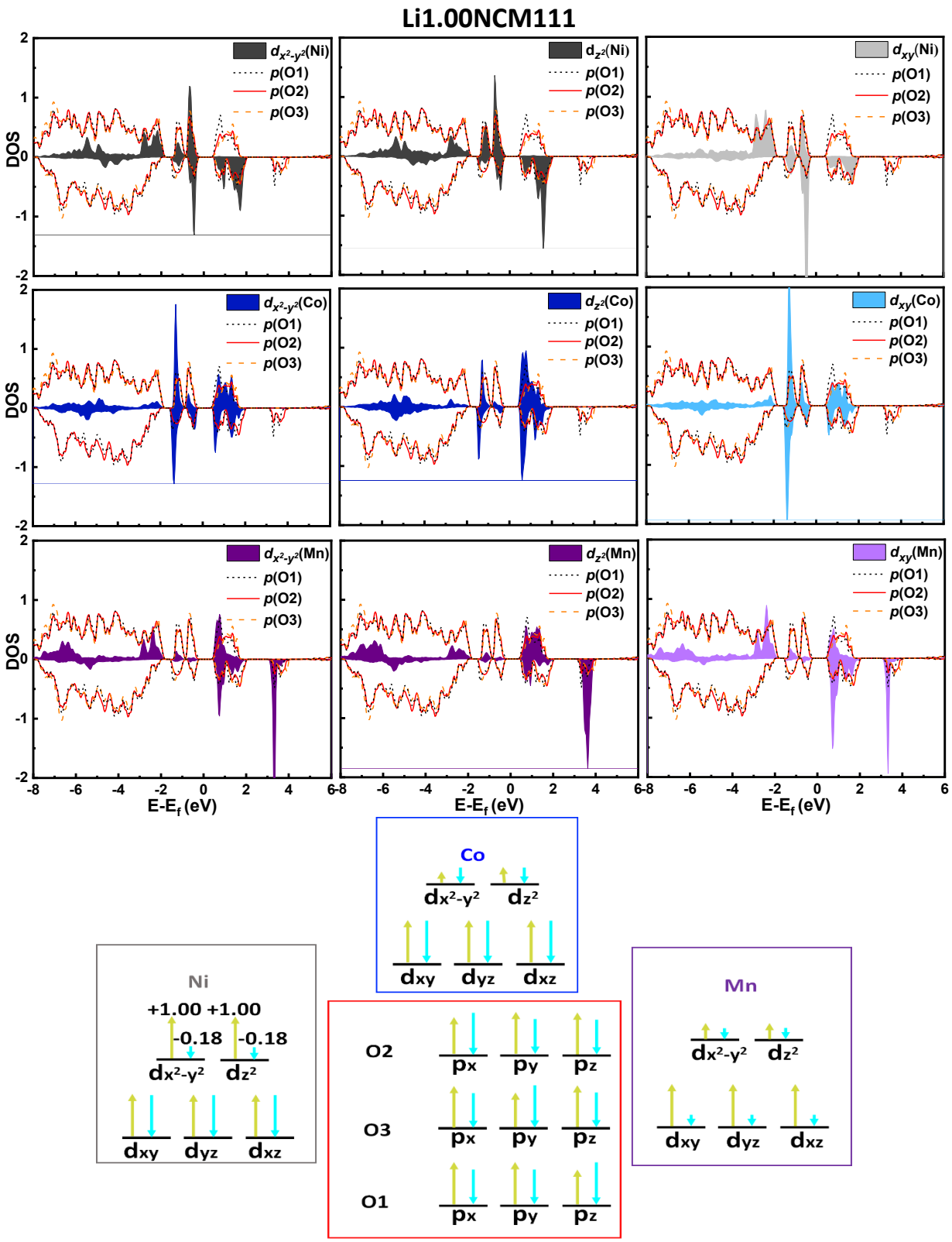

Fig. S5. Partial density of states (PDOSs) and proposed electronic configurations in the most favorable Li1.00NCM111 structures based on DFT-SCAN calculation. The atomic coordinates were rotated about the by-axis to align axial TM–O bonds (in TMO_6 octahedra) along the global *z*-axis of the unit cell to assign the e_g and representative t_{2g} states.

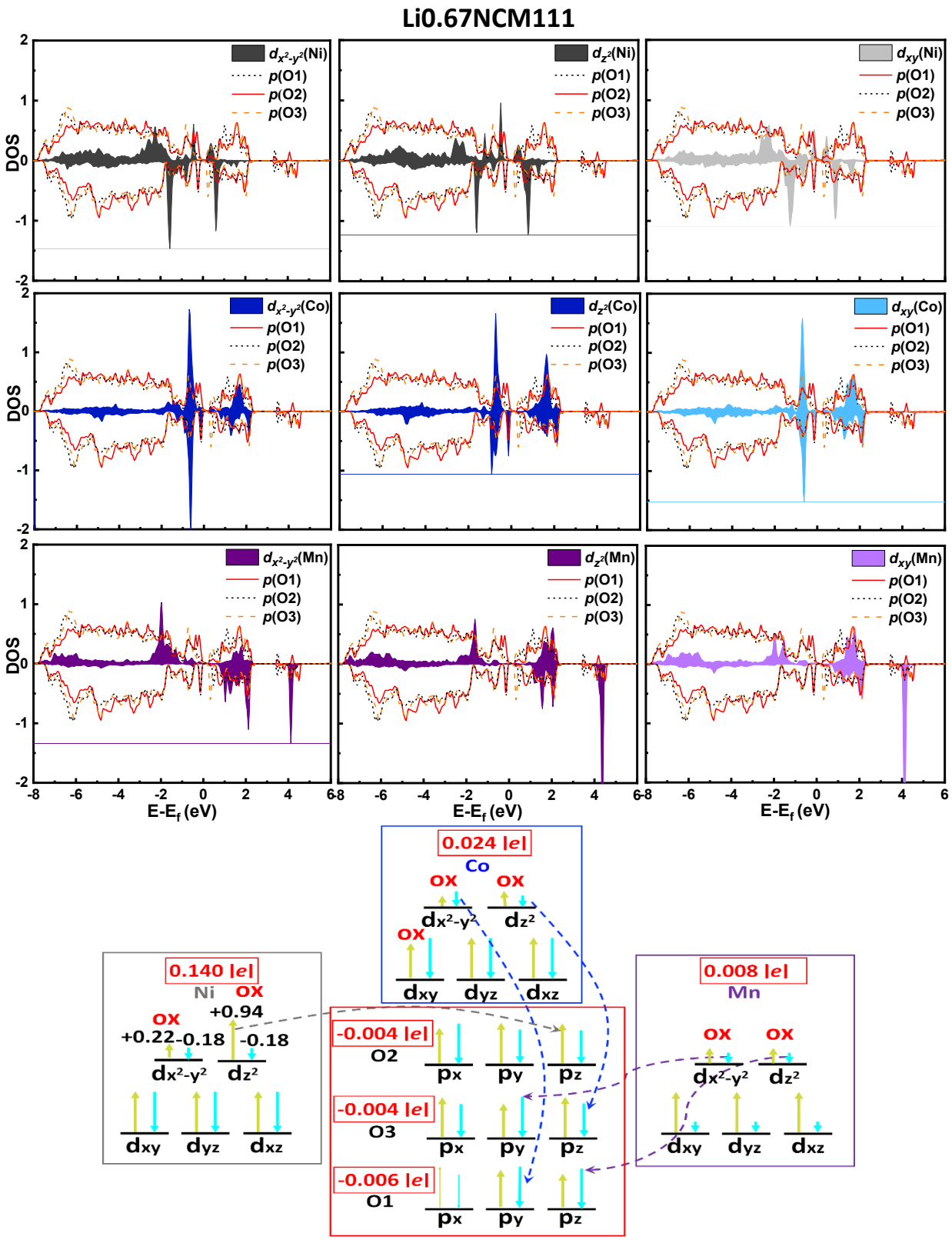

Fig. S6. Partial density of states (PDOSs) and proposed electronic configurations in the most favorable Li0.67NCM111 structures based on DFT-SCAN calculation. The atomic coordinates were rotated about the by-axis to align axial TM–O bonds (in TMO_6 octahedra) along the global *z*-axis of the unit cell to assign the e_g and representative t_{2g} states.

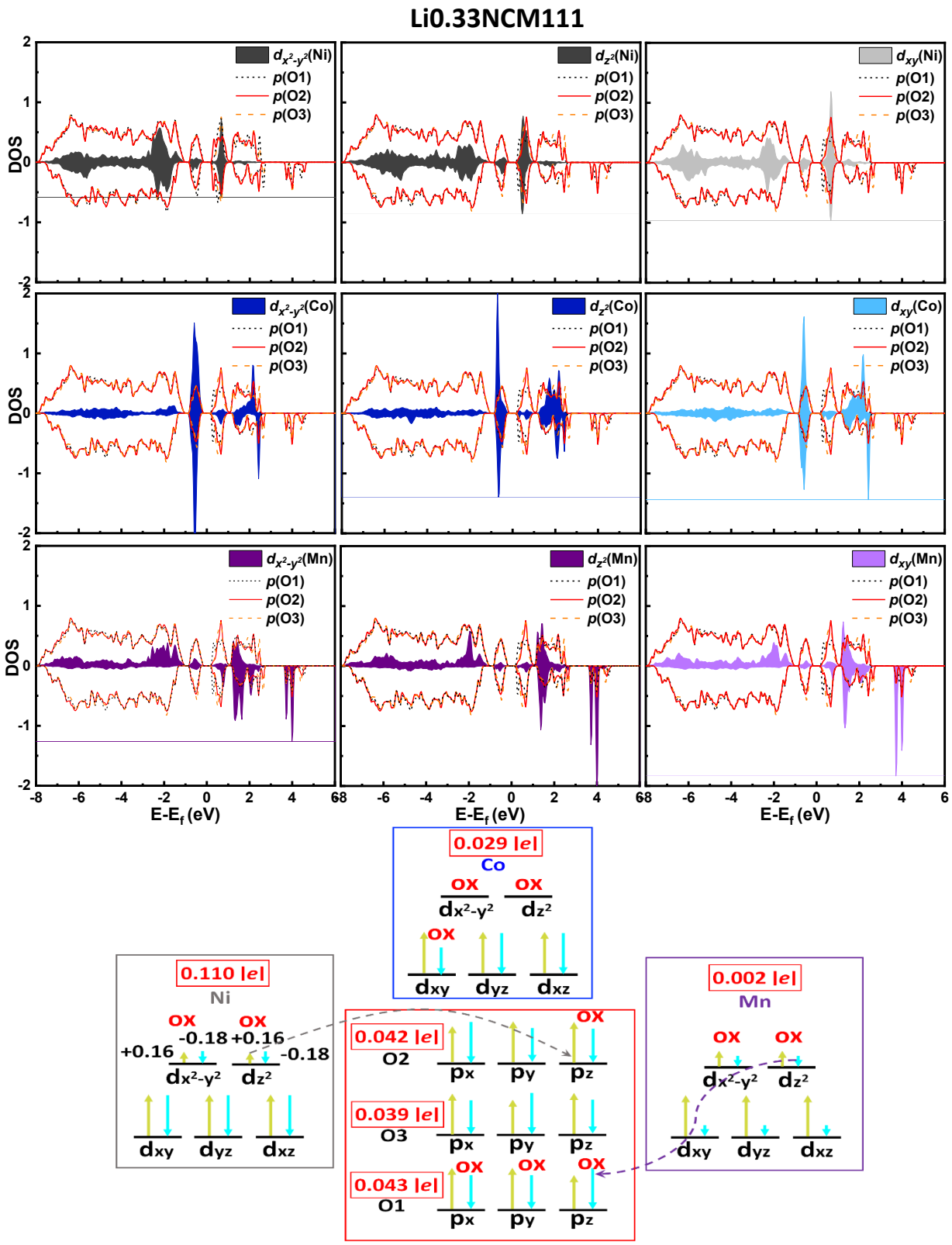

Fig. S7. Partial density of states (PDOSs) and proposed electronic configurations in the most favorable Li0.33NCM111 structures based on DFT-SCAN calculation. The atomic coordinates were rotated about the by-axis to align axial TM–O bonds (in TMO_6 octahedra) along the global *z*-axis of the unit cell to assign the e_g and representative t_{2g} states.

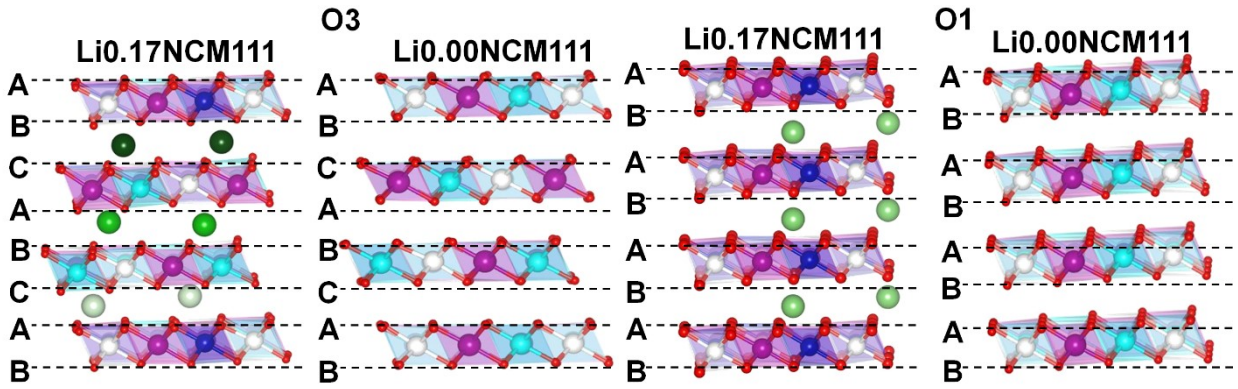

Figure S8. Calculated atomic structures and stacking of Li0.17NCM111 and Li0.00NCM111 structures in O3 and O1 phases using the SCAN functional.

	Bader charge [e^-]					E_C [eV]
	Li	Ni	Co	Mn	O	
O3	-	1.406	1.504	1.755	−0.778	−777.73
O1	-	1.494	1.617	2.017	−0.855	−931.28
	formal charge [e^-]					
O3	-	4	4	4	−2	−5126.13
O1	-	4	4	4	−2	−5064.89

Table S2. Calculated Coulomb energies (E_c) for O3 and O1 phases of Li0.00NCM111 using calculated averaged Bader charges (DFT-SCAN).